# GRACE gravity data target possible mega-impact in north central Wilkes Land, Antarctica

Ralph R.B. von Frese[1,2], Laramie V. Potts[2,1], Stuart B. Wells[1], Luis R. Gaya-Piqué[3,1],

Alexander V. Golynsky[4], Orlando Hernandez[5,1], Jeong Woo Kim[6,1], Hyung Rae Kim[7],

Jong Sun Hwang[8,1], and Patrick T. Taylor[7]


[1]Dept. of Geological Sciences & Byrd Polar Research Center, The Ohio State University,

   Columbus, OH 43210  USA

[2]Laboratory for Space Geodesy & Remote Sensing Research, The Ohio State University,

   Columbus, OH 43210  USA

[3]Istituto Nazionale di Geofisica e Vulcanologia, Rome, ITALY

[4]VNIIOkeangeologia, Dept. of Antarctic Geology, St. Peterburg, RUSSIA

[5]Dept. of Geosciences, Universidad Nacional de Colombia, Bogotá, D.C. COLOMBIA

[6]Dept. of Geoinformation Engineering, Sejong University, Seoul, KOREA

[7]NASA Geodynamics Branch, Goddard Space Flight Center, Greenbelt, MD 20771  USA

[8]Dept. of Earth System Sciences, Yonsei University, Seoul, KOREA

ABSTRACT

A prominent positive GRACE satellite-measured free-air gravity anomaly over regionally depressed subglacial topography may identify a mascon centered on ($70^{o}$S, $120^{o}$E) between the Gamburtsev and Transantarctic Mountains of East Antarctica. Being more than twice the size of the Chicxulub crater, the inferred Wilkes Land impact crater is a strong candidate for a Gondwana source of the greatest extinction of life at the end of the Permian. Its ring structure intersects the coastline and thus may have strongly influenced the Cenozoic rifting of East Antarctica from Australia that resulted in the enigmatic lack of crustal thinning on the conjugate Australian block.

INTRODUCTION

Analysis of earthquake surface waves observed at the Wilkes (now Casey) Station during the 1957-58 International Geophysical Year (IGY) suggested that thinner-than-normal continental crust underlies as much as a quarter of the Antarctic ice sheet (1). Subsequent radio-echo and seismic soundings of the ice sheet revealed the regionally depressed subglacial topography in **Figs. 1.A** and **1.B** for the northern half of East Antarctica between the Gamburtsev and Transantarctic Mountains that includes Lake Vostok (2; 3). Analysis of the depressed terrain's gravity effects indicated that the Moho here may be roughly 7 km shallower than in the rest of East Antarctica (4). The conjugate Australian block apparently lacks complementary crustal thinning (5), thus making it difficult to attribute the thinned Antarctic crust solely to the effects of Cenozoic Gondwana rifting.

Satellite geopotential field observations significantly augment the extremely limited geological and geophysical constraints on the enigmatic crustal properties of Wilkes Land. For example, satellite free-air gravity anomalies observed by the Gravity Research and Climate Experiment (GRACE) mission (**Fig. 2.A**) and their first vertical derivatives (**Fig. 2.B**) show a well defined anomaly maximum over the large subglacial crater in **Fig. 1** centered on (70°S, 120°E) in north central Wilkes Land. Inverse correlations of crater topographies and positive satellite free-air gravity anomalies on the Moon define uncompensated concentrations of enhanced mass or "mascons" (e.g., 6; 7; 8). The mascon is commonly attributed to uncompensated components of the crater's mare fill and/or to the presence of an underlying mantle plug that the rebounding crust produced on meteorite impact. The strength of the lithosphere presumably supports these excess masses in the crust to produce the free-air gravity maximum.

As far as we are aware, the Wilkes Land crater is the first mascon detected in the Earth's gravity field at satellite altitudes. Its subglacial topographic signature has a diameter of roughly 350 km along 70°S latitude and 500 km along 120°E longitude. The entire state of Ohio can fit within this enormous central crater. It is more than twice the size of the Chicxulub crater in Mexico's Yucatán Peninsula and somewhat larger than the South African Vredefort crater.

The Chicxulub crater has nearly achieved isostatic equilibrium since the Cretaceous-Tertiary impact because its small mascon gravity signal (9) is apparent only at airborne altitudes. The Precambrian Vredefort crater also lacks a mascon gravity signal at satellite altitudes, suggesting that it developed in ancient lithosphere that was

considerably warmer and weaker than the Moon's which has maintained mascons for over 3.5 Ga. These results suggest to us that the Wilkes Land mascon may be much younger than the Vredefort impact whose enormous mass is still seeking to approach the isostatic equilibrium of the smaller Chicxulub mascon.

No additional evidence for meteorite impact in Wilkes Land is apparent, although early studies had inferred an impact crater in northwestern Wilkes Land (10). In 1959-60, the U.S. Victoria Land Expedition had obtained data during an oversnow traverse of an immense negative free-air gravity anomaly and several seismic ice thickness estimates that were interpreted as a giant meteorite crater at roughly (71.5°S, 139.5°E). However, this interpretation was abandoned when subsequent airborne radio-echo soundings showed no evidence of the presumed crater (11).

The recent discovery of chondritic meteorite fragments in rocks of the Permian-Triassic boundary in Antarctica and Australia (12) sparked a hunt for Gondwana impact(s) that may have obliterated about 90% of the Earth's species roughly 250 million years ago. Seismic, gravity, and drill-core data have identified the Bedout High off the northwestern coast of Australia as a possible Late Permian impact structure that is roughly the size of Chicxulub (13).

We offer the inferred Wilkes Land impact crater (WLIC) as another possible candidate, although the paucity of geological and near-surface geophysical data clearly limits our ability to determine its detailed crustal properties. However, in the following sections, we develop a crustal model for the WLIC that may be tested by long-range

aerogeophysical surveying (14) and studies of the glacial deposits along the Wilkes Land coastline.

CRUSTAL MODELING

The central basin inferred from the subglacial topography in **Fig. 1.B** has a relative depth of roughly 0.7 km. Although subsequent erosion and sedimentation undoubtedly modified the crater's topography, its signature remains relatively well preserved through time as the result of the enhanced susceptibility of the impact-fractured crust to glacial erosion (e.g., 15).

The free-air gravity anomalies in **Figs. 2.A** and **2.B** were derived at 200-km altitude from the satellite-only GRACE gravity model (16) evaluated to spherical harmonic degree and order 90. These model parameters were chosen to emphasize the more robust qualities of the GRACE measurements. For example, the model's covariance properties indicate that the higher frequency components are relatively poorly determined. At lower altitudes, the anomaly estimates also have dramatically increasing noise levels, as well as decreasing reliability due to the lack of terrestrial or airborne gravity observations (4) and the lack of uniqueness of the gravity modeling (17).

The inferred mascon's free-air signature in **Fig. 2.A** consists of the well defined relatively positive 7-mGal anomaly overlying the basin that is further resolved in the first vertical-derivative gravity-anomalies of **Fig. 2.B**. To evaluate the inferred mascon's first order crustal properties, we computed the spherical coordinate gravity effects of the terrain's ice, water, and subglacial rock components at 20 km altitude by Gauss-Legendre

quadrature integration (4). Subtracting these terrain gravity effects from the zero free-air anomaly yielded complete Bouguer anomalies that we related by inversion entirely to Moho variations. The black profile in **Fig. 3.E** gives these Moho estimates along 70°S. Specifically, our modeling assumed that the horizontal density contrast of 0.5 g/cm$^3$ between mantle and crust fully compensated the basin's crust across the Moho.

Along 70°S in **Fig. 3.E**, the inferred mantle plug is some 9-km thick and 350-km across. These spatial dimensions are probably minimal because erosion and sedimentation have muted the subglacial topography. However, the associated prominent satellite free-air anomaly (**Fig. 3.B**) suggests that the crustal model may not be completely compensated. Therefore, we adjusted the inferred Moho to nullify the free-air anomaly for the equilibrium Moho given by the red profile in **Fig. 3.B**, while the white-shaded difference between the two Mohos in **Fig. 3.E** estimates the possible mascon. Computing the mascons's gravity effect at 5-km altitude reveals the well defined 15-mGal anomaly in **Fig. 3.C** that long-range aerogravity surveying could readily test.

Impacts such as Chicxulub are also known to modify crustal magnetization significantly (18). Unfortunately, only the two aeromagnetic profiles in **Fig. 4** sample the crustal magnetizations of the WLIC. Collected during the 1957-58 IGY on flights between Byrd and Wilkes Stations (19), the profiles are anti-correlated and thus appear severely contaminated by external field effects. However, the tendency for strong anomaly maxima and gradients to overlie the inferred rings suggests that important new

insights concerning the crustal properties of the WLIC would result from modern aeromagnetic surveying.

DISCUSSION

Our crustal modeling suggests that the white-shaded mantle component in **Fig. 3.E** can account for the mascon of the inferred WLIC. The diameter $D_1$ of its central basin ring as inferred from the subglacial topography is more than twice the 180-km central basin diameter of Chicxulub that the legend of **Fig. 1.B** compares to scale. Large multi-ring basins of the Moon and other terrestrial planets appear to follow the $D_n = (\sqrt{2})^{n-1} D_1$ ring spacing rule for the diameter $D_n$ of the $n^{th}$-ring (20). By this rule, the Wilkes Land coastline roughly intersects the northern margin of second ring as shown in **Fig. 1**.

This result raises the interesting possibility that meteorite-impacted crust influenced the Cenozoic rifting of Australia from Antarctica. This idea helps to account for the enigmatic one-sided nature of the crustal thinning in East Antarctica relative to the normal thickness of the Australian crust that the impact and rifting left largely intact. It also provides a minimum age constraint on the impact that accordingly must have occurred at or before the Cenozoic breakup of Australia and East Antarctica.

As a maximum age constraint, the WLIC appears to be younger than any of the large Precambrian multi-ring impact basins like Vredefort that essentially lack satellite altitude free-air gravity anomalies. This age constraint is consistent with the relatively prominent GRACE free-air anomaly of the WLIC which infers a lesser state of isostatic

equilibrium in the underlying crustal components than apparently occurs for the older crust of the Precambrian impacts.

The above timing considerations may very broadly constrain the age of the WLIC to between the Late Precambrian and Cenozoic. However, the enormous size of the impact most certainly would have profoundly affected the development of life. An especially noteworthy event occurred near the end of the Permian Period when some 90% of marine life and nearly 75% of terrestrial life on Earth was obliterated. This greatest known mass extinction of all time some 250 Ma ago has been associated with the effects of flood basalt volcanism in the Siberian Traps (21), global lowering of sea level (22), and a large Gondwana impact (12). While the marine Bedout High off the northwestern coast of Australia might represent a Chicxulub-sized Permian event (13), the much larger WLIC is clearly another prime Gondwana impact candidate. The WLIC is also antipodal to the Siberian Traps in Permian continental reconstruction coordinates, and may have disrupted mass from crust to core much like the large multi-ring basin impacts apparently did on the Moon (7).

These results suggest that an enormous meteorite impact may have greatly affected the geological and tectonic setting of the northern half of East Antarctica between the Gamburtsev and Transantarctic Mountains including subglacial Lake Vostok. Unfortunately, other than partial coverage from radio-echo and seismic soundings of the subglacial topography, essentially no geological and near-surface geophysical data are available to constrain the crustal properties of the inferred WLIC. The U.S. National Science Foundation (NSF), however, is developing a dedicated ski-

equipped long-range research aircraft that can map the subglacial topography, gravity, and magnetic anomalies of this remote region (14). These observations together with studies of glacial deposits along the coast for evidence of a meteorite impact are necessary to refine the properties of the enigmatic ice-covered crust of north central Wilkes Land.

## CONCLUSIONS

Seismic surface wave dispersion studies from Wilkes Station in the 1957-58 IGY first identified the enigmatic crustal thinning of the East Antarctic continent. Subsequent ice-penetrating radio-echo and seismic soundings revealed regionally depressed subglacial topography in the northern half of East Antarctica between the Gamburtsev and Transantarctic Mountains, while the related terrain gravity effects indicated significantly thinner underlying crust than in the rest of the continent. The highest resolution gravity coverage of the region from the GRACE satellite mission reveals a prominent free-air gravity maximum over the large subglacial oblong depression centered on ($70^{o}$S, $120^{o}$E) in north central Wilkes Land.

This inverse correlation of basin topography with an overlying satellite free-air gravity maximum characterizes lunar impact craters known as mascons. The Wilkes Land crater terrain gravity effects are consistent with an underlying roughly 425-km wide, 9-km thick mantle plug produced by crustal rebound from meteorite impact. However, the GRACE free-air anomaly of the Wilkes Land mascon suggests that no

more than about 90% of the mantle plug's mass may be isostatically compensated at the Moho.

The inferred WLIC is more than twice the size of the Chicxulub crater, and thus a strong candidate for a Gondwana source of the greatest extinction of life at the end of the Permian. Its ring structure intersects the coastline, and thus it may have predated and strongly influenced the Cenozoic rifting of Australia from East Antarctica. This impact scenario also helps explain the enigmatic lack of crustal thinning on the conjugate Australian block.

In summary, the occurrence of an enormous Permo-Triassic impact in north central Wilkes Land is consistent with meteorite evidence in the comparably aged Gondwana rocks, as well as the regionally disrupted and thinned crust of East Antarctica between the Gamburtsev and Transantarctic Mountains, which includes a huge 500 km by 350 km subglacial depression overlain by a well-defined GRACE free-air gravity maximum. The lack of geological and near-surface gravity, magnetic and other geophysical data clearly limits our interpretation of the timing and crustal properties of the WLIC.

Our gravity modeling, in particular, is not unique and thus can not exclude the possibility that the mascon reflects the presence of basalt flows, or a gabbro intrusive, or some other regional high-density body beneath the basin. However, checking the glacial deposits along the Wilkes Land coast and geophysical surveying using NSF's proposed long-range airborne mapping capability can critically test our inferred crustal model for the WLIC.

REFERENCES AND NOTES

1.  F. Press and G. Dewart, *Science* **129**, 462 (1959).

2.  D.J. Drewry, *Antarctica: Glaciological and Geophysical Folio* **sheet 3**, (Scott Polar Research Institute, Cambridge University, 1983).

3.  BEDMAP url: http://www.antarctica.ac.uk/aedc/bedmap/

4.  R.R.B. von Frese et al., *J. Geophys. Res.* **104**, 25275 (1999).

5.  G. Clitheroe, O. Gudmundsson, and B.L.N. Kennett, *J. Geophys. Res.* **105**, 13697 (2000).

6.  D.U. Wise and M.T. Yates, *J. Geophys. Res.* **75**, 261 (1970).

7.  L.V. Potts and R.R.B. von Frese, *J. Geophys. Res.* **108**, 5024 (2003).

8.  L.V. Potts and R.R.B. von Frese, *J. Geophys. Res.* **108**, 5037 (2003).

9.  V.L. Sharpton et al., *Science* **261**, 1564 (1993).

10. J.G. Weihaupt, *J. Geophys. Res.* **81**, 5651 (1976).

11. C.R. Bentley, *J. Geophys. Res.* **84**, 5681 (1979).

12. A.R. Basu et al., *Science* **302**, 1388 (2003).

13. L. Becker et al., *Science* **304**, 1469 (2004).

14. M. Studinger et al., *Eos (Trans. Am. Geophys. Un.)* **86**, 39 (2005).

15. B. Dent, *GSA Bull.* **84**, 1667 (1973).

16. B.D. Tapley et al., *Geophys. Res. Lett.* **31**, 10.1029/2004GL019920 (2004).

17. R.R.B. von Frese et al., in C. Reigber, H. Lühr, and J. Wickert (eds.), *Earth Observation with CHAMP* (Springer Verlag, Berlin, p. 287, 2005).

18. G.T. Penfield and A. Camargo-Zanoguera, *Soc. Explor. Geophys.* **51**, 37 (1981).

19. N.A. Ostenso and E.C. Thiel, *Aeromagnetic Reconnaissance of Antarctica Between Byrd and Wilkes Stations* **Res. Rep. 64-6**, (Geophysical and Polar Research Center, The University of Wisconsin, 1964).

20. P.D. Spudis, The *Geology of Multi-Ring Impact Basins*, (Cambridge University Press, New York, p. 277, 2005).

21. P.R. Renne and A.R. Basu, *Science* **253**, 176 (1991).

22. P.D. Ward, D.R. Montgomery, and R. Smith, *Science* **289**, 1740 (2000).

23. Elements of this research were produced with support from the Office of Polar Programs of the National Science Foundation under research grant NSF-OPP 0338005 and The Ohio Supercomputer Center at The Ohio State University.
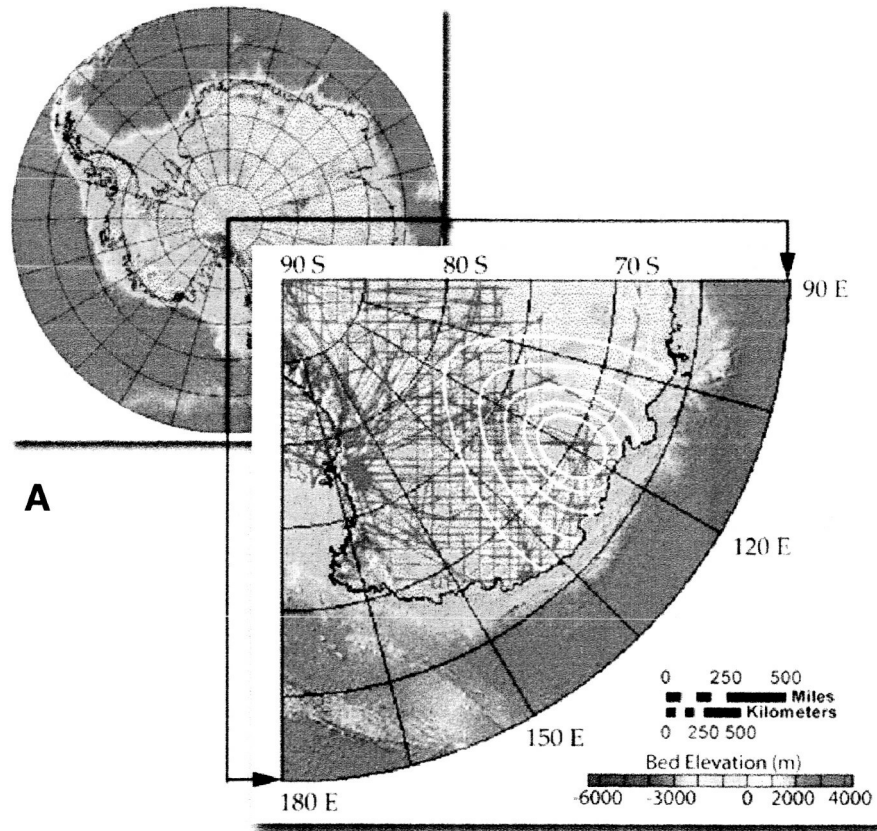
**Fig. 1. (A)** Shaded bathymetry and subglacial topography of Antarctica south of 60°S with the insert of the study region showing the coverage (red lines) by airborne radio-echo and seismic soundings (2; 3) superimposed on the partial ring structure (white contours) of the inferred Wilkes Land impact crater. **(B)** Expanded view of the bathymetry and subglacial topography of the study region. For comparison, the Chicxulub crater is given to scale in the legend. The bold dotted line shows the profile considered in **Fig. 3** along 70°S.

**Fig. 2. (A)** GRACE satellite free-air gravity anomalies and **(B)** their first vertical derivatives at 200 km altitude. The bold dotted line shows the profile considered in **Fig. 3** along 70°S.

**Fig. 3.** Crustal modeling along the 70°S profile segment highlighted in **Figs. 1** and **2** that crosses the inferred Wilkes Land impact basin. **(A)** First vertical derivatives (FVD) of the **(B)** GRACE (red profile) free-air gravity anomalies (FAGA) at altitude (Z) with the mean value of -6.42 mGals removed. The black profile shows the mascon's modeled effects and the grey shading delineates the rings that cross the profile. **(C)** The modeled gravity effects at airborne altitude (Z) of the mascon defined by the white-shaded region in **E**. **(D)** Cross-section of the ice and subglacial elevations that were modeled for their gravity effects at 20 km altitude. **(E)** Cross-section of the lower crust and upper mantle where the black profile gives the Moho inferred from the gravity effects of **C** assuming that the mass differentials across this Moho completely compensate the terrain. The red-lined Moho is the black-lined Moho adjusted to account for the GRACE free-air anomaly

in **B**. The white-shaded difference between the two Mohos gives the mass excess with gravity effects in **B** (black profile) that account for the GRACE free-air gravity anomalies and also predicts the strong airborne gravity signal in **C**.

**Fig. 4.** Aeromagnetic profiles (A-A') and (B-B') collected during the 1957-58 IGY superposed on the subglacial topography and inferred ring structure of the WLIC.
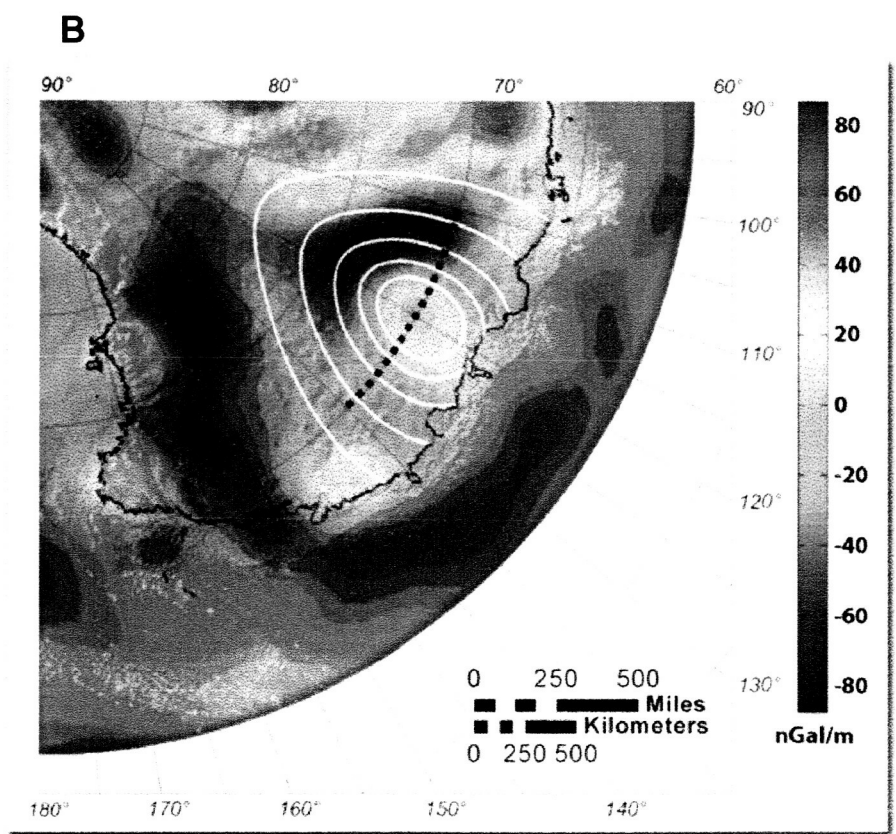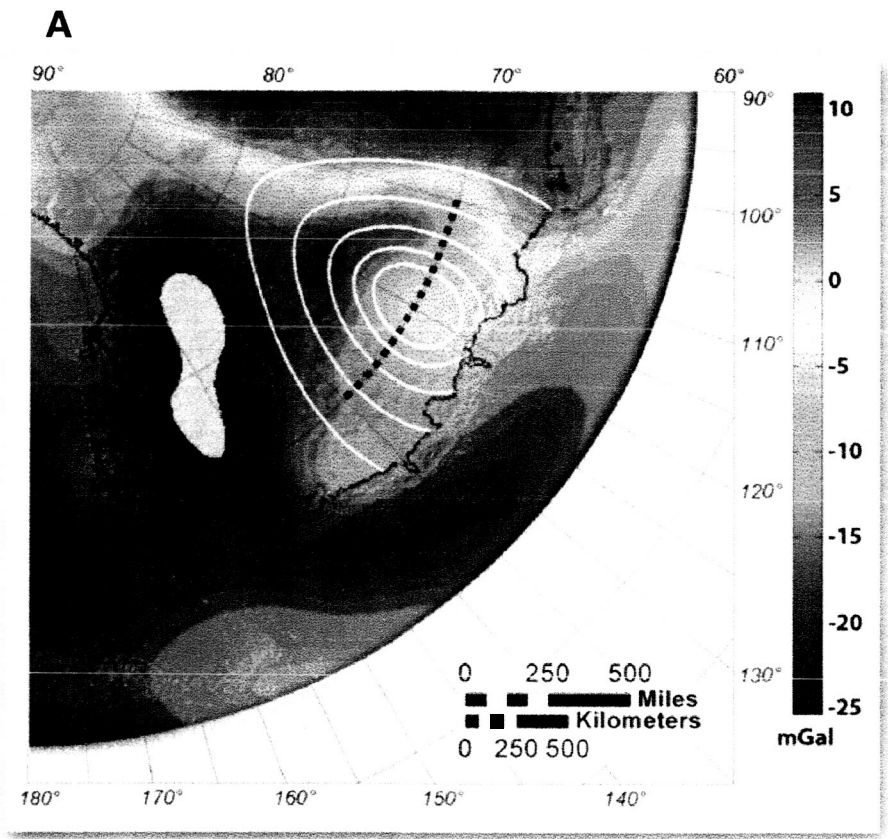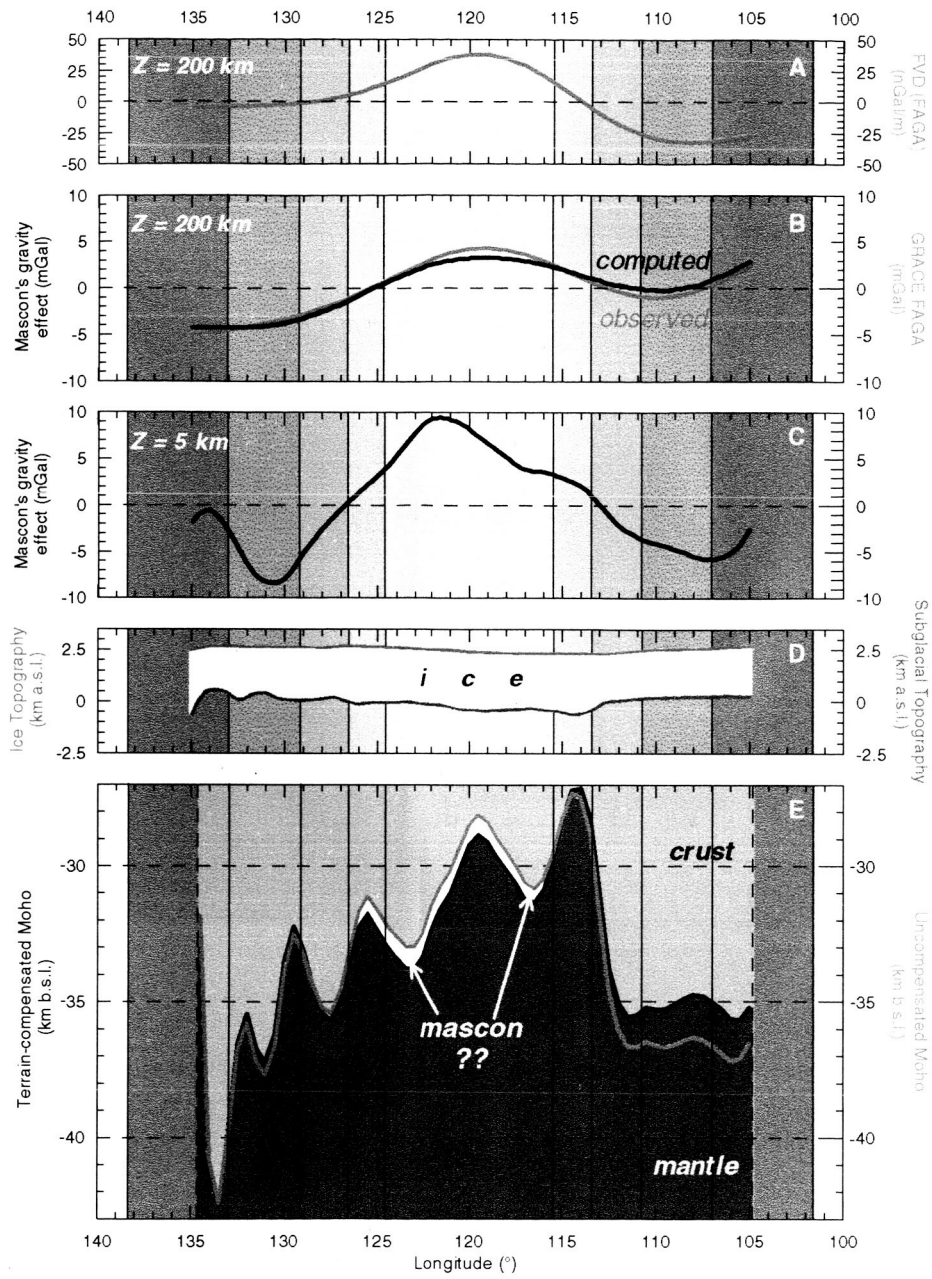
**A**

**B**

Chicxulub
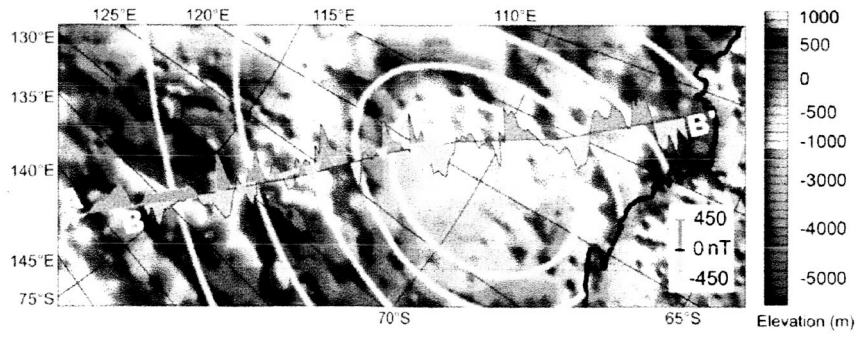
**Figure 1**

**A**

**B**
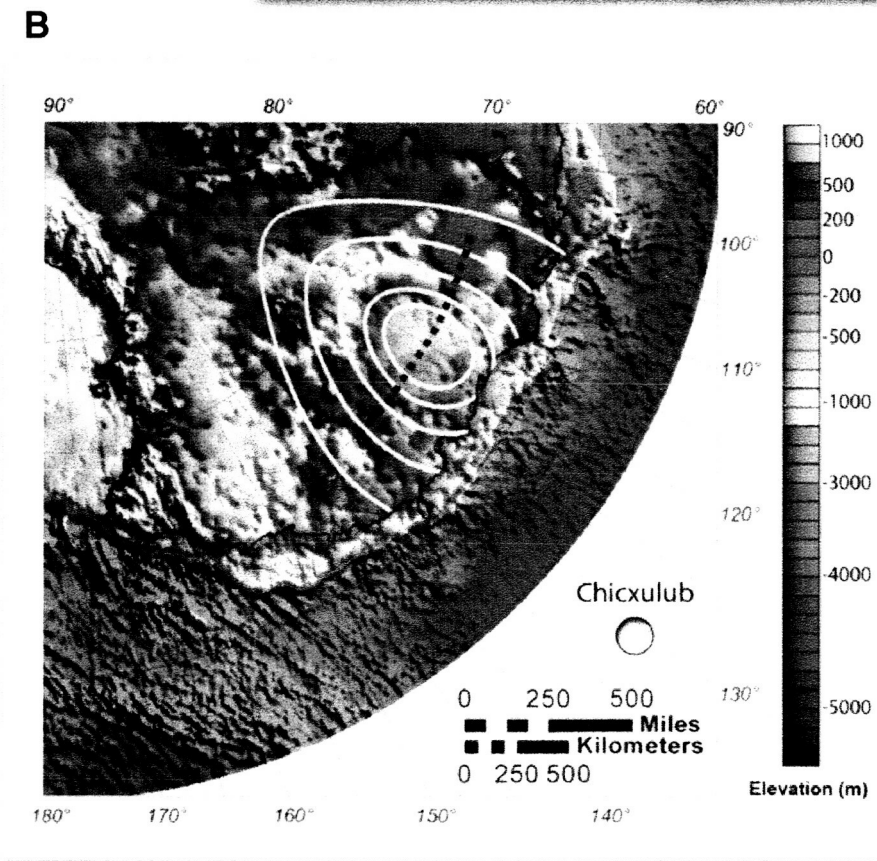
**Figure 2**

**Figure 3**

**Figure 4**